V International Conference on Simulation for Additive Manufacturing
Sim-AM 2025
F. Auricchio, M. Carraturo and S. Morganti (Eds)

ANALYTICAL INVESTIGATION OF GLOBAL AND LOCAL INSTABILITY IN ADDITIVELY MANUFACTURED LATTICE-CORE SANDWICH COLUMNS

S. OSMANOGLU*, A. NAIR † AND C. MITTELSTEDT†

*Institute for Lightweight Engineering and Structural Mechanics (LSM), Technical University of Darmstadt
Otto-Berndt-Str. 2, 64287 Darmstadt, Germany
e-mail: serhat.osmanoglu@lsm.tu-darmstadt.de

†Institute for Lightweight Engineering and Structural Mechanics (LSM), Technical University of Darmstadt, Germany

Key words: sandwich column, lattice-core structure, additive manufacturing, global instability, local instability, analytical modeling, finite element

Abstract. This paper analytically investigates global and local instability in sandwich columns with monolithic aluminium facesheets and Face-Centered Body-Centered Cubic (FBCC) lattice cores produced by additive manufacturing. To account for core transverse compressibility and its influence on face local instability characterized by wrinkling, a higher-order solution is developed. Finite Element simulations using 3D solid elements for the facesheets and beam elements for the core under various boundary conditions validate the model. Analytical and numerical results show close agreement, accurately predicting global (in-plane/out-of-plane) and local (intracell/wrinkling) modes. Boundary conditions strongly affect global instability, whereas local instability depends mainly on geometric parameters. The proposed method offers an efficient and accurate tool for predicting instability in lattice-core sandwich columns for lightweight structural applications.

1 INTRODUCTION

Additive manufacturing (AM) enables the production of lightweight lattice-core sandwich structures with tunable mechanical properties. These configurations offer high stiffness-to-weight ratios and design flexibility, allowing control over strength and energy absorption through unit cell geometry. Using Selective Laser Melting (SLM), fully integrated sandwich columns can be fabricated without adhesive bonding, ensuring uniform load transfer and defect-free interfaces. Previous studies on various lattice topologies, including BCC, FCC, and FBCC, have examined global and local buckling behavior, highlighting the strong influence of geometry and boundary conditions.[1–5] However, only a limited number of analytical studies have addressed local instability phenomena in additively manufactured lattice-core sandwich structures. The developed model introduces a higher-order analytical framework for lattice-core sandwich columns to accurately predict both global and local instabilities. The proposed model, validated through FEM simulations, provides improved accuracy and computational efficiency for design applications.

2 MATERIALS AND DESIGN

The sandwich column was designed for additive manufacturing from AlSi10Mg using the Laser Selective Melting (LSM) process. As shown in Fig. 1, the facesheets and FBCC lattice core were considered to be printed simultaneously, ensuring a continuous, defect-free interface without adhesive bonding. The effective core properties were evaluated using the analytical model of Xia et al.,[6] which links the equivalent elastic moduli and Poisson's ratios to the strut-to-cell ratio and base material properties, and validated by FEM.[7]

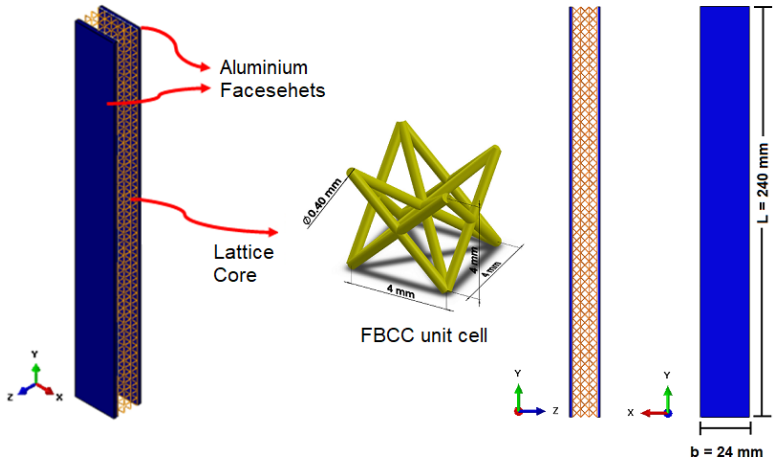

Figure 1: Geometry of the sandwich column with FBCC lattice core. All unit cells have dimensions of $4 \times 4 \times 4$ mm and strut diameter $d_s = 0.4$ mm.

3 ANALYTICAL METHODS FOR BUCKLING PREDICTIONS

Global buckling represents the overall instability of a sandwich column under axial compression, where deformation occurs along the weaker bending axis, while local buckling (face instability) is confined to limited regions such as the faces or core. Depending on the stiffness distribution, either out-of-plane or in-plane global buckling may dominate, as described by Allen's thin–thick face model,[8] which accurately incorporates facesheet bending stiffness and shear deformation effects. Local modes include intracell buckling and wrinkling; the former occurs within individual lattice cells, and the latter develops over longer wavelengths along the face–core interface. Analytical approaches for these buckling modes are primarily based on the formulations by Allen[8] for global buckling and Zenkert[9] for intracell buckling, both providing reliable predictions of critical loads for lattice-core sandwich structures. The wrinkling solution is addressed in the following section within the scope of this study.

4 HIGHER-ORDER APPROACH FOR FACE WRINKLING

4.1 Model Simplifications

This section presents an energy-based higher-order analytical framework for predicting wrinkling in sandwich columns with FBCC lattice cores. Unlike conventional models assuming uniform transverse displacement, the proposed formulation employs fourth-order axial and third-order transverse variations to capture the core's compressibility and shear effects. This refined representation improves

the accuracy of instability predictions. A closed-form expression for the symmetric wrinkling load is derived using the Ritz method, based on the following key assumptions:

1. The faces are considered relatively thin and follow the Kirchhoff–Love assumption.
2. The core is compressible in the transverse and axial directions.
3. The core displacements must satisfy the following symmetric deformation criteria:

$$u^c(z > 0) = u^c(z < 0) \tag{1a}$$
$$w^c(z > 0) = -w^c(z < 0) \tag{1b}$$

4. The face sheets and the core are assumed to be perfectly bonded.
5. Taking into account the symmetry of wrinkling mode, only the structure lying above the mid-plane is considered for calculating the wrinkling load.

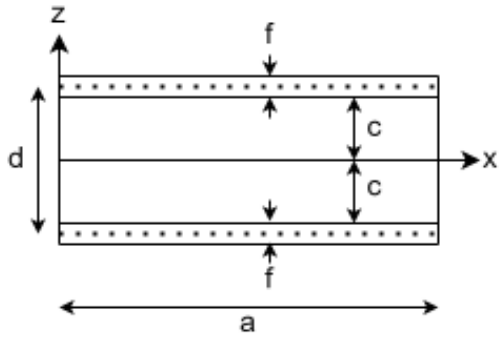

Figure 2: Sandwich Construction

4.2 Kinematic Relations

A sandwich column of length a, core thickness $2c$, and face sheet thickness f is analyzed (Fig. 2). A Cartesian coordinate system is defined at one end with its origin at the core mid-plane. The column is loaded in the x–z plane, inducing displacements u and w in the respective directions. Quantities with subscript 0 refer to the mid-surfaces, and all stiffness and loads are expressed per unit width.

Assuming the face sheets follow Kirchhoff–Love kinematics and are thin compared to the total section, the displacement field for the upper face sheet ($c \leq z \leq c + f$) is :

$$u^t(x, z) = u_0^t(x) - \left(z - c - \frac{f}{2}\right) w_{0,x}^t(x) \tag{2a}$$
$$w^t(x, z) = w_0^t(x) \tag{2b}$$

The only non-zero strain in the face sheet is the axial strain, which is written as

$$\epsilon_{xx}^t(x, z) = u_{,x}^t(x, z) = u_{0,x}^t(x) + \left(c + \frac{f}{2} - z\right) w_{0,xx}^t(x) \tag{3}$$

In sandwich structures, core transverse deformation is often neglected in classical first-order models but becomes significant for compliant cores or under extreme loads such as blasts.[10] To account for this, a higher-order displacement expansion in the transverse coordinate is employed, allowing accurate representation of in-plane and out-of-plane responses. The core displacement field is expressed as:

$$u^c(x,z) = \left(1 - \beta_2 \frac{z^2}{c^2}\right) u_0^c(x) + w_{,x}^c(x) \frac{z}{c} \tag{4a}$$

$$w^c(x,z) = w_0^c(x) \frac{z}{c} + \beta_3 \frac{z^3}{c^3} \tag{4b}$$

In these equations, w_c^0 and u_c^0 are the transverse and in-plane displacement of the middle plane of the core, while β_i (i = 2 and 3) are unknown functions that are to be determined from displacement continuity, as follows:

For the top-face-sheet/core interface, $z = c$,

$$u^c(x,z)\big|_{(z=c)} = u^t(x,z)\big|_{(z=c)} \tag{5a}$$

$$w^c(x,z)\big|_{(z=c)} = w^t(x,z)\big|_{(z=c)} \tag{5b}$$

Substitution of Eqs. (4) into the two continuity equation (10) leads to:

$$\beta_2 = \frac{2u_0^c(x) - 2u_0^t(x) - f w_{0,x}^t(x) + 2w_{0,x}^c(x)}{2u_0^c(x)} \tag{6a}$$

$$\beta_3 = w_0^c(x) - w_0^t(x) \tag{6b}$$

The in-plane displacement in the core is (fourth order in z):

$$u^c(x,z) = u_0^c(x) + \frac{z^2}{c^2}\left(u_0^t(x) - u_0^c(x) + \frac{f\, w_{0,x}^t(x)}{2}\right) - \frac{z^4\left(w_{0,x}^c(x) - w_{0,x}^t(x)\right)}{c^4} \tag{7a}$$

Thus, the transverse displacement in the core in this new higher-order core theory can be expressed as follows (third order in z):

$$w^c(x,z) = \frac{z w_0^c(x)}{c} - \frac{z^3\left(w_0^c(x) - w_0^t(x)\right)}{c^3} \tag{7b}$$

Accordingly, the formulation involves four generalized variables: the upper facesheet displacements (u_0^t, w_0^t) and the core displacements (u_0^c, w_0^c). Using linear strain–displacement relations, the core deformation is expressed through three strain components: axial ϵ_{xx}^c, transverse ϵ_{zz}^c, and shear γ_{zx}^c, representing in-plane extension, thickness compression, and shear distortion, respectively. These strains form the basis for the total strain energy of the sandwich column.

4.3 Constitutive Framework

The derived formulations apply to materials of any type. For the following analysis, the facesheets are assumed isotropic and the core transversely isotropic. The notation $1 \equiv x$, $3 \equiv z$, and $55 \equiv zx$ is used. Under these assumptions, the constitutive relations for the facesheets are expressed as:

$$\sigma_{xx}^t = C_{11}^t \, \epsilon_{xx}^t, \tag{8a}$$
$$\sigma_{zz}^t = C_{13}^t \, \epsilon_{xx}^t. \tag{8b}$$

Note that σ_{zz}^t is excluded from the variational formulation, as its associated strain ϵ_{zz}^t equals zero. The constitutive relation for the core is then expressed as:

$$\begin{bmatrix} \sigma_{xx}^c \\ \sigma_{zz}^c \\ \tau_{zx}^c \end{bmatrix} = \begin{bmatrix} C_{11}^c & C_{13}^c & 0 \\ C_{13}^c & C_{33}^c & 0 \\ 0 & 0 & C_{55}^c \end{bmatrix} \begin{bmatrix} \epsilon_{xx}^c \\ \epsilon_{zz}^c \\ \gamma_{zx}^c \end{bmatrix} \tag{9}$$

The stiffness matrix C_{ij}^c in Eq. (9) can be also defined as the inverse of the compliance matrix, whose coefficients depend on the elastic and shear moduli and the Poisson's ratios of the core material.

4.4 Governing Formulation

The governing equation for the buckling of the sandwich column is derived from the principle of minimum potential energy and solved using the Ritz method. The total potential energy Π in the buckled configuration is expressed as the sum of the internal strain energy Π_i and the external load potential Π_a:

$$\Pi = \Pi_i + \Pi_a \tag{10}$$

The internal and external potentials were substituted into the total potential energy expression in Eq. (10) to evaluate the critical buckling load. The Ritz method was then applied to minimize the total potential energy and obtain an approximate solution.[11,12] Simply supported shape functions were adopted because wrinkling is effectively independent of boundary constraints, as Allen[8] assumed an infinitely long column. This variational expression represents the equilibrium criterion for the onset of buckling. The strain energy or inner potential stored in the buckled column can be calculated as follows:

$$\Pi_i = \int_0^L \left[\int_c^{c+f} \sigma_{xx}^t \epsilon_{xx}^t \, \mathrm{d}z + \int_0^c (\sigma_{xx}^c \epsilon_{xx}^c + \sigma_{zz}^c \epsilon_{zz}^c + \tau_{zx}^c \gamma_{zx}^c) \, \mathrm{d}z \right] \mathrm{d}x \tag{11}$$

At the onset of buckling, the applied load P produces a lateral displacement w. The total load is divided between the face sheet and the core as $F^t P$ and $F^c P$, such that both layers undergo the same axial strain $\epsilon_{xx}^t = \epsilon_{xx}^c$.

The facesheets and the core are aligned longitudinally in parallel, ensuring consistent strain distribution across both elements. The mathematical expressions explicating this correlation are presented subsequently. Taking into account Hook's law $\sigma = E\epsilon$ and $\sigma = \frac{F}{A}$ and taking into account the forces

and interactions of the isolated system :

$$P = F^t P + F^c P \tag{12a}$$

$$F^t = \frac{2E^f f}{E_1^c c + 2E^f f} \tag{12b}$$

$$F^c = \frac{E_1^c c}{E_1^c c + 2E^f f} \tag{12c}$$

$$\Pi_a = -\frac{P}{2}\int_0^L \left(F^t \left(\frac{dw^t}{dx}\right)^2 + F^c \left(\frac{dw^c}{dx}\right)^2 \right) dx \tag{12d}$$

$$\Pi_a = -\frac{P}{2\left(E_1^c c + 2E^f f\right)}\int_0^L \left(2E^f f \left(\frac{dw^t}{dx}\right)^2 + E_1^c c \left(\frac{dw^c}{dx}\right)^2 \right) dx \tag{12e}$$

The internal and external potential expressions were substituted into the variational form of the total potential energy given in Eq. (10) to compute the critical buckling load. The Ritz method, which minimizes the total potential energy, was employed to obtain an approximate solution.[11,12] Since wrinkling occurs as if it were infinitely far from the edges, it is considered insensitive to end constraints; therefore, simply supported shape functions were adopted.

$$u_0^j(x,z) = U^j \cos\frac{n\pi x}{a} \tag{13a}$$

$$w_0^j(x,z) = W^j \sin\frac{n\pi x}{a} \tag{13b}$$

where j denotes either t or c. The shape functions given in Eq. (13) are substituted into the total elastic potential of the column. The remaining variables subject to variation are the Ritz constants U^j and W^j. Accordingly, the first variation of the total potential energy becomes:

$$\delta\Pi = \frac{\partial\Pi}{\partial U^t}\delta U^t + \frac{\partial\Pi}{\partial U^c}\delta U^c + \frac{\partial\Pi}{\partial W^t}\delta W^t + \frac{\partial\Pi}{\partial W^c}\delta W^c = 0 \tag{14}$$

Because the variations of the constants are independent, Eq. (14) is satisfied when

$$\frac{\partial\Pi}{\partial U^t} = \frac{\partial\Pi}{\partial U^c} = \frac{\partial\Pi}{\partial W^t} = \frac{\partial\Pi}{\partial W^c} = 0 \tag{15}$$

These are the Ritz equations—a homogeneous system from which the unknown constants U^j and W^j are obtained. For the critical buckling load P, the equations can be written in matrix form as

$$\underline{\underline{K}}\,\underline{U} = 0 \tag{16}$$

where $\underline{\underline{K}}$ is a 4×4 stiffness matrix depending on P and the sandwich parameters, and $\underline{U} = [U^t\ U^c\ W^t\ W^c]^T$ is the vector of Ritz constants.

$$\det|\underline{\underline{K}}| = 0 \tag{17}$$

This eigenvalue problem yields multiple buckling loads, with the smallest eigenvalue representing the critical buckling load P.

5 FINITE ELEMENT ANALYSIS

Finite element analyses were performed in ABAQUS/CAE to validate the analytical buckling predictions. A 3D linear perturbation buckling study using the subspace algorithm was conducted, modeling the facesheets with quadratic solid (C3D20R) and the lattice core with beam (B31) elements. Tie constraints ensured continuous bonding, replicating the monolithic structure. Boundary conditions constrained both ends, and compressive loading was applied through reference nodes for uniform load transfer. Mesh refinement continued until critical load convergence. The final model, with a $20\,\text{mm}$ core and $3\,\text{mm}$ facesheets (6–12 elements through thickness), accurately captured global buckling and local wrinkling under various end conditions, as shown in Fig. 3.

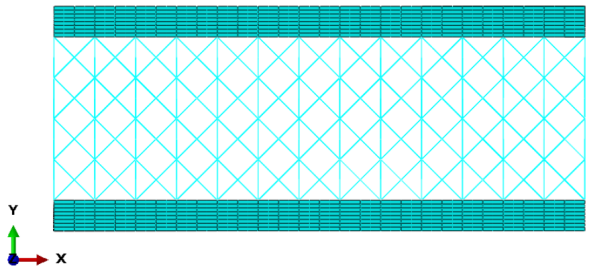

Figure 3: Representative meshed section of the sandwich column.

6 RESULTS

This section presents the global and local buckling results of lattice-core sandwich columns. A higher-order analytical model, derived from wrinkling analysis, is validated through FEM simulations for core thicknesses of 8–$24\,\text{mm}$ and facesheet thicknesses of 0.25–$4\,\text{mm}$, with fixed cell size ($4\,\text{mm}$) and strut diameter ($0.4\,\text{mm}$). The analytical predictions are consistent with FEM results under various boundary conditions, demonstrating the robustness of the proposed model.

6.1 Comparison of the Comprehensive Analytical Model

A unified analytical framework is established by integrating the proposed wrinkling formulation with the classical theories of Allen[8] and Zenkert,[9] which describe global and intracell buckling, respectively. The combined model evaluates the critical loads of all potential instability modes and determines the dominant one corresponding to the lowest critical value.

Once the formulation is established, it enables the calculation of the critical buckling load for a given sandwich structure configuration. Additionally, it determines the failure mode associated with the lowest critical load among the following types: out-of-plane buckling (P_O), in-plane buckling (P_I), intracell buckling (P_D), and wrinkling (P_W). The critical load for the structure is given by the following:

$$P \leq \min\left[P_O, P_I, P_D, P_W\right] \tag{18}$$

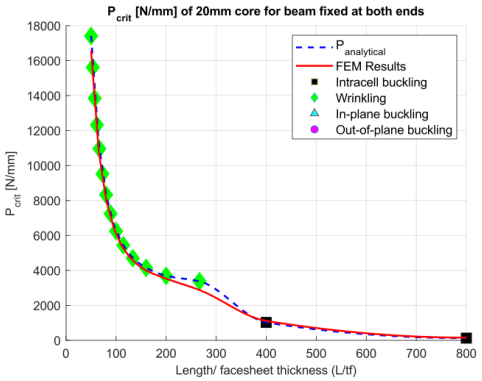

(a) Result for 20mm core of Fixed-Fixed column

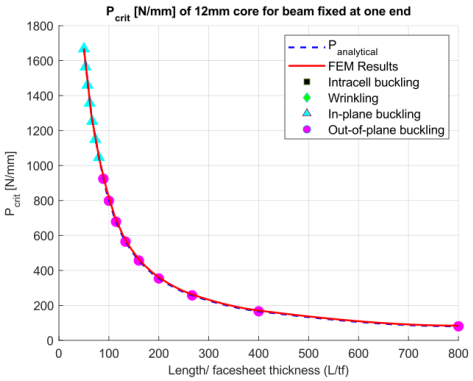

(b) Result for 12mm core of Fixed-Free column

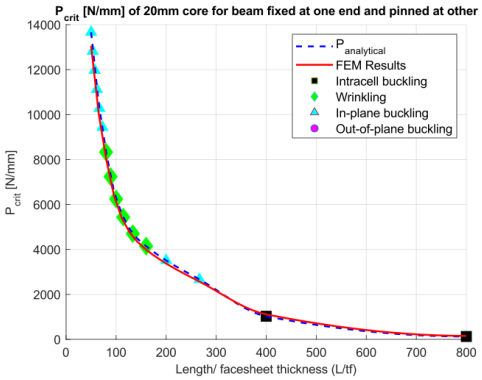

(c) Result for 20mm core of Fixed-Pinned column

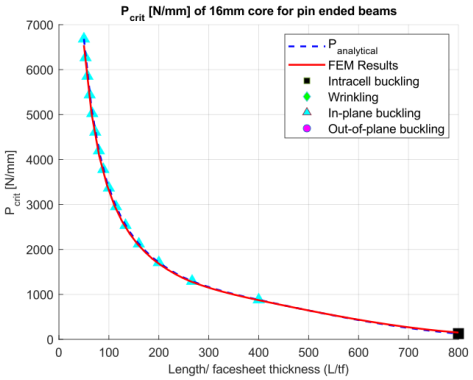

(d) Result for 16mm core of Pinned-Pinned column

Figure 4: Comparison of final analytical solution for FBCC with FEM results for each boundary condition.

Fig. 4 presents a comparative analysis between the proposed analytical model and FEM results under various boundary conditions. For each case, a representative core thickness was selected to capture the range of buckling modes observed.

Intracell buckling was identified for thin facesheets (0.25–0.5 mm) under all boundary conditions except fixed–free, as shown in Figs. 4a, 4c, and 4d. The corresponding deformation mode is illustrated in Fig. 5b, confirming that this instability occurs only when the facesheets are sufficiently thin.

Wrinkling, on the other hand, is primarily governed by the material and geometric characteristics of the faces and core rather than by boundary conditions. The deformation pattern for a column with a 20 mm core and 2 mm facesheets under fixed–fixed supports is shown in Fig. 5a. As seen in Figs. 4a–4c, wrinkling occurs at relatively low L/t_f ratios and remains almost unaffected by the applied boundary conditions. The analytical predictions closely follow the FEM results, confirming that the proposed higher-order formulation accurately captures the wrinkling response across different configurations.

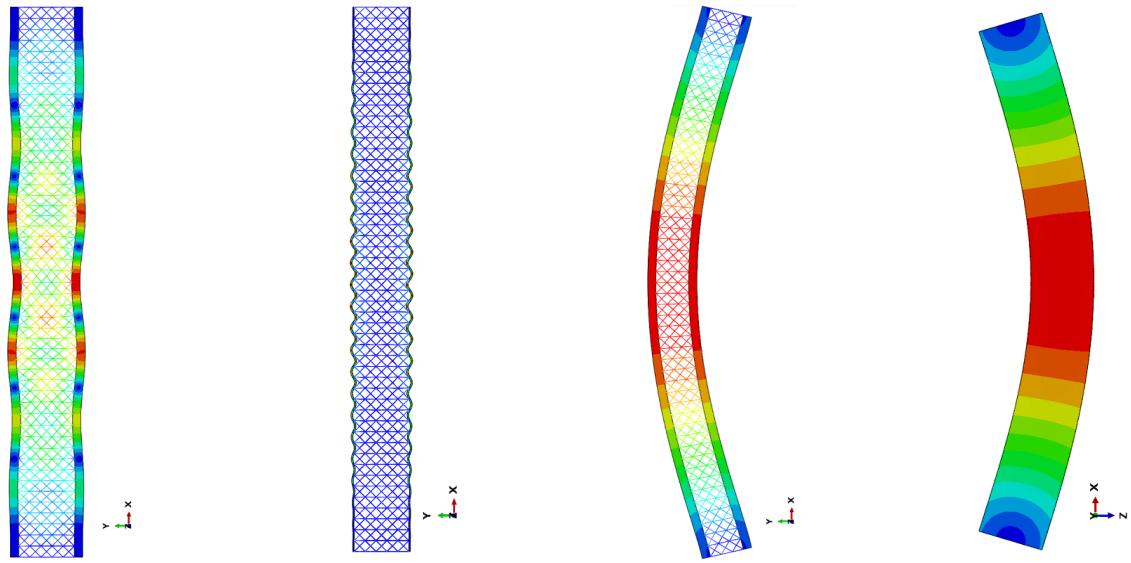

(a) (b) (c) (d)

Figure 5: (a) Wrinkling, (b) Intracell buckling, (c) Out-of-plane buckling, and (d) In-plane buckling in sandwich columns.

Global buckling was observed in the form of out-of-plane and in-plane buckling as shown in Fig. 5c and 5d. In-plane buckling primarily occurs when the stiffness about the z-axis is weaker than that of the y-axis. However, stiffness is not the sole governing parameter. In the current configuration, in-plane buckling was observed only under Fixed-Free and Pinned-Pinned boundary conditions. In some instances like Fig. 4c, the buckling mode transitioned from in-plane buckling to wrinkling. This observation highlights that both the stiffness characteristics of the sandwich column and the boundary conditions significantly influence the buckling mode. While it is commonly assumed that buckling is more likely to occur along the axis with weaker stiffness, the results indicate that this assumption does not always hold.

7 CONCLUSIONS

A comprehensive investigation was conducted on the overall and localized buckling behavior of sandwich columns with FBCC lattice cores. Global instability was assessed using classical formulations, while a refined higher-order analytical approach was developed to predict wrinkling, constituting the main contribution of this work. The global response, analyzed in both in-plane and out-of-plane directions, followed the weaker stiffness axis, and Allen's formulation[8] was adopted for its effective treatment of thin and thick core configurations. Local instabilities, namely intracell buckling and wrinkling, were assessed using Zenkert's relation[9] and the proposed higher-order wrinkling model. Finite element comparisons confirmed strong agreement, accurately capturing the shift between global and local modes. The proposed formulation provided results consistent with FEM in a fraction of the computational time, emphasizing its suitability for efficient design analyses.

REFERENCES

[1] Tochukwu George, V. Deshpande, and Haydn N. G. Wadley. Mechanical response of carbon fiber composite sandwich panels with pyramidal truss cores. *Composites Part A-applied Science*

and Manufacturing, 47:31–40, 2013.

[2] R. Umer, Z. Barsoum, HZ Jishi, Kuniharu Ushijima, and W.J. Cantwell. Analysis of the compression behaviour of different composite lattice designs. *Journal of Composite Materials*, 52:715 – 729, 2018.

[3] Hussam Georges, Wilfried Becker, and Christian Mittelstedt. Analytical and numerical analysis on local and global buckling of sandwich panels with strut-based lattice cores. *Archive of Applied Mechanics*, 2024.

[4] Xiaoyang Wang, Lei Zhu, Liao Sun, and Nan Li. Optimization of graded filleted lattice structures subject to yield and buckling constraints. *Materials & Design*, page 109746, 2021.

[5] He Zhang, Yu kun Liu, Xiao hong Wang, Tao Zeng, Zhi xin Lu, and Guo dong Xu. Global buckling behavior of a sandwich beam with graded lattice cores. *Journal of Sandwich Structures & Materials*, 26:317 – 335, 2023.

[6] Huanxiong Xia, Junfeng Meng, Jianhua Liu, Xiaohui Ao, Shengxiang Lin, and Ye Yang. Evaluation of the equivalent mechanical properties of lattice structures based on the finite element method. *Materials*, 15(9), 2022.

[7] Serhat Osmanoglu and Christian Mittelstedt. Global buckling response of sandwich panels with additively manufactured lattice cores. *Journal of Sandwich Structures & Materials*, 2024.

[8] Howard G. Allen. *Analysis and design of structural sandwich panels*. Pergamon Press Ltd, Oxford, 1969.

[9] Dan Zenkert. An introduction to sandwich structures, 1995.

[10] Renfu Li and George A Kardomateas. Nonlinear high-order core theory for sandwich plates with orthotropic phases. *AIAA journal*, 46(11):2926–2934, 2008.

[11] B. K. Hadi and F. L. Matthews. Development of benson–mayers theory on the wrinkling of anisotropic sandwich panels. *Composite Structures*, 49(4):425–434, 2000.

[12] Riccardo Vescovini, Michele d'Ottavio, Lorenzo Dozio, and Olivier Polit. Buckling and wrinkling of anisotropic sandwich plates. *International Journal of Engineering Science*, 130:136–156, 2018.